

Structural Phase Transition in CdSb + 3 % MnSb Composite at a High Hydrostatic Pressure

R.G. Dzhamamedov¹, A.Ju. Mollayev^{1,*}, A.V. Kochura², P.V. Abakumov², R.K. Arslanov¹,
S.F. Marenkin^{3,4}, M.B. Dobromyslov⁵

¹ *Amirkhanov Institute of Physics, Dagestan Scientific Center, Russian Academy of Sciences,
94, Yaragского St., 367003 Makhachkala, Dagestan, Russia*

² *South-West State University, Regional Centre of Nanotechnology,
94, 50 let Otyabrya St., 305040 Kursk, Russia*

³ *Institute of General and Inorganic Chemistry of Russian Academy of Sciences,
31, Leninskii Pr., 119991 Moscow, Russia*

⁴ *Moscow Institute of Steel and Alloys (National University of Science and Technology),
4, Leninskii Pr., 119049 Moscow, Russia*

⁵ *Pacific National University, 136, Tikhookeanskaya St., 680035 Khabarovsk, Russia*

(Received 02 October 2015; published online 24 December 2015)

In CdSb + 3 % MnSb composite, structural properties have been studied, specific resistance ρ and Hall coefficient R_H are measured at a high hydrostatic pressure of up to $P \leq 9$ GPa. An irreversible structural phase transition is found at barometric dependencies $\rho(P)$ and $R_H(P)$. From our experimental data, barometric dependencies of carrier concentration and their mobility are calculated. On the basis of the heterophase structure – effective medium model, characteristic points and parameters of the phase transition, and also dynamics of variation of the initial phase volume C_1 as a function of pressure are computed. The latter dependence is in agreement with the investigation results of Raman scattering before and after application of pressure.

Keywords: Magnetic composite, Cadmium antimonide, Spintronic materials, Hydrostatic pressure, Transport properties

PACS numbers: 81.40.Rs, 81.40.Vw, 75.50.Pp,
78.30.Hv

1. INTRODUCTION

Semiconducting compounds doped with 3d-metals are the promising materials for magnetoelectronics (spintronics) [1]. Depending on the doping element, its atoms can both replace the cation vacancies in a base semiconductor and form interstitial defects. In this case, the state of a diluted magnetic semiconductor is implemented. However, if the limit of solubility is surpassed, phase layering in the lattice of a base semiconductor may occur, which results in the formation of micro- or nanoscale magnetic inclusions (clusters). Diluted magnetic semiconductor $\text{In}_{1-x}\text{Mn}_x\text{Sb}$ with nanoscale inclusions of ferromagnetic semimetal MnSb with Courrier temperature of around 600 K [2] is an example when both cases given above are realized. A similar situation occurs for semiconductors of the group $A^{\text{II}}B^{\text{V}}$, where $B = \text{Sb}$, doped with manganese. The present work continues that research [5-8] at high hydrostatic pressures up to 9 GPa.

Earlier, in works [7, 8], undoped single crystal samples p -CdSb were studied. The samples were oriented along crystallographic directions [001] (sample No 1) and [010] (sample No 2). Specific electrical resistance ρ and Hall coefficient R_H was measured at high hydrostatic pressure $P \leq 7$ GPa at elevation and drop off of pressure within the range of room temperatures. At dependencies $\rho(P)$ and $R_H(P)$, structural phase transitions were found. In sample No 1, a reversible semiconductor-semiconductor phase transition was observed and in sample No 2 an irreversible phase transition accompanied by the matter decomposition occurred. X-ray study

of the samples after loading has shown that the deformed sample No 1 oriented along [001] produced at Laue pattern continuous rings with sharp maxima – polycrystal with texture. For sample No 2, the swing curve consisted from a number of peaks that corresponded to the reflection off individual blocks. Relative disorientation of these blocks was ~ 1 - 1.50° , indicating considerable impairment of the sample quality.

We have investigated structural and electrical properties of composite sample CdSb + 3 % MnSb at a high hydrostatic pressure of up to 9 GPa in the range of room temperature.

2. EXPERIMENTAL DETAILS

Original crystals were prepared with directional crystallization according to Bridgeman from polycrystal CdSb + 3 % MnSb ingots, which were produced beforehand by alloying of antimonides cadmium and manganese. The samples were cut from the central part of the crystal and then underwent chemical-mechanical polishing with abrasive particles whose size was not greater than 20 nm.

To examine the sample structure, the composition and element distribution at the surface, scanning electron microscope (SEM) JSM-6610LV (Jeol) with attachment for energy dispersive X-ray spectroscopy (EDXS) X-MaxN (Oxford Instruments) was used. Spectra of Raman scattering (RS) were measured at room temperature with the use of combined system with confocal fluorescent spectrometer and RS spectrometer OmegaScopeTM (AIST-NT Inc.) featuring laser wavelength of 532 nm,

* a.mollaev@mail.ru

power of 50 mW. The spot of a focused light at the sample surface was around 500 nm in diameter. The spectral resolution was 0.8 cm^{-1} .

The installation for measuring kinetic coefficients at hydrostatic pressures $P \leq 9 \text{ GPa}$ was a high-pressure device such as toroid [9], which was upgraded to concurrently measure several kinetic coefficients.

In order to concurrently measure specific resistance and Hall effect a many-turn solenoid [10] was used, which made it possible to produce a magnetic field $H \leq 5 \text{ kOe}$. A fluoroplastic capsule with a volume of $\approx 80 \text{ mm}^3$ was applied as a working cell, which had 12 electric inputs. That made it possible to measure specific resistance, Hall effect, and control pressure at compression and decompression. A manganin manometer was calibrated by using fixed points (Bi, Tl, etc.) Samples were prepared as parallelepipeds with sizes of $2.8 \times 0.7 \times 0.5 \text{ mm}$. As a medium transferring pressure, a mixture of methanol and ethanol (4 : 1) hydrostatic up to 10 GPa was used [11]. To determine to what extent the medium was hydrostatic, two identical single-crystal samples *n*-Ge with $\rho = 1.75 \Omega \cdot \text{cm}$ were put in a measuring cell perpendicular to each other. The quantity ρ was measured as a function of pressure up to 9 GPa at 300 K. Both samples revealed that at a fixed pressure the values of specific resistance did not coincide when the pressure was elevated and lowered. This fact indicates that there were not axis strengths that had been observed earlier in the range 4-5 GPa when as a transfer medium *n*-pentane-isoamyl alcohol was used. In addition to that, these data about dependence $R(P)$ corroborate that the pressure was rather hydrostatic and shear stresses were absent.

Contacts for measuring electrical properties were made by soldering with solders at the basis of tin. The error in measuring resistance, Hall effect and pressure was not greater than $\pm 3\%$, 3.5% and 3% , respectively.

3. RESULTS AND DISCUSSION

Typical images of the sample surface obtained with SEM are given in Fig. 1.

Clearly seen are defects of the sample structure as cracks and volume inclusions with a nonhomogeneous distribution. These inclusions are both of point and needle-like shape with the smallest side of $0.5\text{-}1 \mu\text{m}$. EDXS has revealed that the areas without defects consisted only of Cd and Sb atoms in virtually equal proportions. Within the area of inclusions in EDXS spectra, peaks were appeared corresponding to Mn atoms.

Distribution maps of Cd, Sb, Mn in the area with inclusions (Fig. 2) measured with EDXS demonstrate the excessive content of Mn in the areas where there are fewer Cd atoms. In doing so, the distribution of Sb atoms is more uniform with a little more content in the areas where many Mn atoms occur. Therefore, inclusions most likely present the phase of $\text{MnSb}_{1+\delta}$ ($\delta > 0$), as it was found earlier in eutectic compositions InSb-MnSb [12]. It should be noted that $\text{MnSb}_{1+\delta}$ is a ferromagnetic semimetal with the highest Currier temperature (T_C) among compounds Mn-V that reaches 585 K for MnSb [13]. In this case, a decrease in Sb content ($\delta < 0$) results in a decrease in T_C [14], whereas at $\delta > 0$ T_C does not change [12].

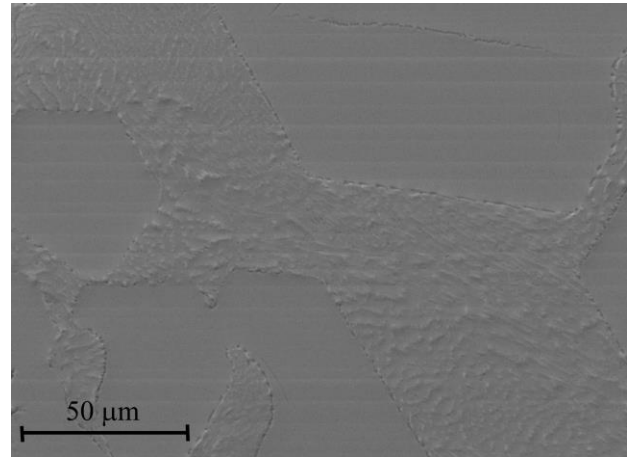


Fig. 1 – SEM image of the sample surface for CdSb + 3% MnSb

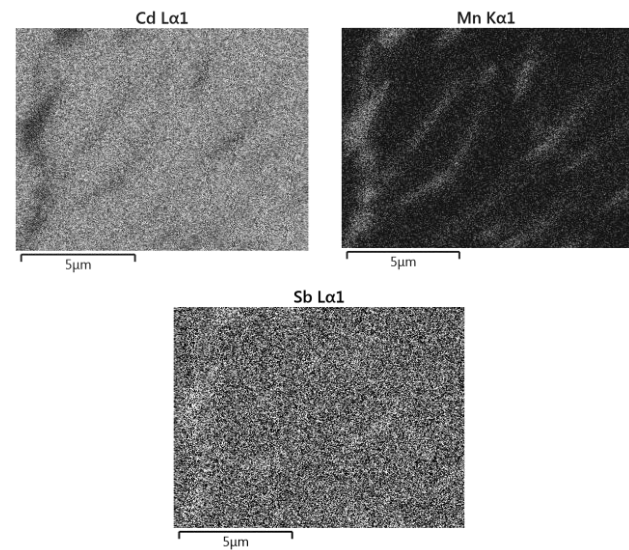


Fig. 2 – Element distribution at the fraction of the sample surface for CdSb + 3% MnSb having inclusions. Image for Sb content is provided after graphical processing in order to compare areas where the content of Sb is little excessive, big Mn content and the absence of Cd

The samples under investigation, therefore, should most likely have ferromagnetic properties with $T_C \approx 585 \text{ K}$.

Crystal lattice of CdSb belongs to the orthorhombic system (spatial group $Pbca$) and has 16 atoms in the elementary cell. In Γ point of the Brillouin zone, 48 normal vibration modes stand out [15]:

$$\Gamma = 6(A_g + B_{1g} + B_{2g} + B_{3g} + A_u + B_{1u} + B_{2u} + B_{3u})$$

of which 24 are RS-active. Earlier, at experimental study of RS-spectra for single crystals CdSb, 22 modes were found: A_g (37.5, 53, 61, 82, 107 and 173 cm^{-1}); B_{1g} (53, 66 and 178 cm^{-1}); B_{2g} (53, 107 and 179 cm^{-1}) and B_{3g} (49, 61, 70, 128, 154 and 171 cm^{-1}) [16].

Raman spectra of CdSb + 3% MnSb sample before application of 8 GPa pressure and after that are shown in Fig.3. Because of features of the experimental device, one was able to measure them only at $\omega > 100 \text{ cm}^{-1}$. In this region, one can see a number of phonon modes of CdSb with a small increase in their frequency (not more

than $1\text{-}2\text{ cm}^{-1}$) compared to the values given above for an undoped single crystal. This fact is in agreement with the results of [17] where such frequency change of phonons was explained by the replacement of Cd atoms with lighter Zn atoms. For CdSb + 3 % MnSb sample, the situation is most likely similar and part of Mn atoms replaces Cd atoms, forming this way solid solution of $\text{Cd}_x\text{Mn}_{1-x}\text{Sb}$. At Raman spectra of the sample before and after pressure application identical modes are observed. However, the spectrum intensity after pressure application is reduced; oscillator strength changes and a broad weak maximum appears around 200 cm^{-1} . Thus, the sample crystallinity was likely lowered and it went a partial phase layering. There was irreversible phase transition, which is indicated by the fact that after pressure application the Raman spectrum amplitude is decreased.

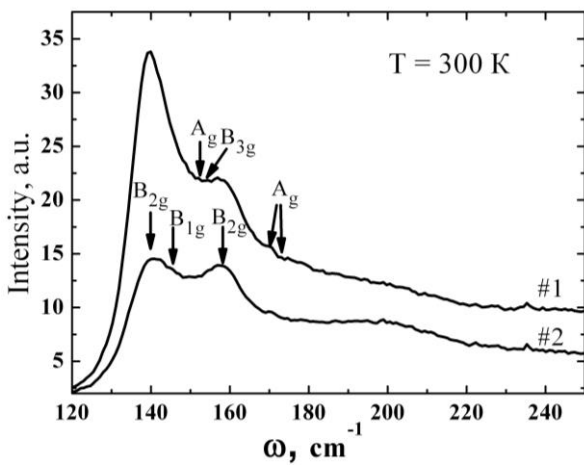


Fig. 3 – Raman spectra for CdSb + 3 % MnSb sample: #1 – before 8GPa pressure application; #2 – after application. Arrows indicate phonon modes observed at both spectra

Experimental barometric dependencies of specific resistance ρ and the Hall coefficient R_H are given in Fig. 4a. Barometric dependencies of carrier concentrations $p(P)$ and mobility $\mu(P)$ at room temperatures calculated with consideration for ρ and R_H for the composite CdSb + 3 % MnSb are depicted in Fig. 4b.

It is seen from Fig. 4a that specific resistance is almost constant up to pressure $P \approx 1.2\text{ GPa}$ and then increases three-fold. At a pressure about 2 GPa, resistance reaches its maximum and then begins to decrease with various barometric coefficients and turns lower by almost 2 orders of magnitude. In the saturation region, specific resistance equals $\rho \approx 7.4 \cdot 10^{-5}\text{ Ohm}\cdot\text{cm}$, i.e. metal conductivity occurs. Whereas at atmospheric pressure $\rho \approx 0.1\text{ Ohm}\cdot\text{cm}$, i.e. semiconductor-to-metal phase transition takes place.

At depressurization, specific resistance at $P \approx 1\text{ GPa}$ is virtually constant but then increases. Initial values of resistance before and after load application are not the same, which is indicative of the fact that irreversible structural phase transition occurred accompanied by the partial layering of phases. At depressurization, hysteresis is observed, which is typical for first-order phase transitions.

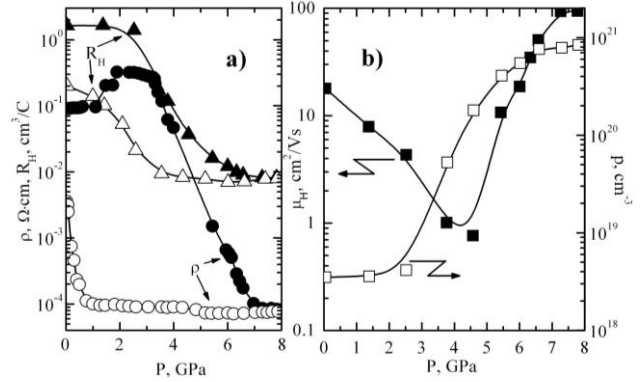


Fig. 4 – Barometric dependencies: a) of reduced to atmospheric pressure specific resistance and Hall coefficient (black symbols – increase in pressure, open – depressurization); b) concentration (open symbols) and mobility (black symbols) at pressure elevation

Hall coefficient (Fig. 4a) varies weakly to a pressure $P \approx 2\text{ GPa}$ and then sharply decreases by more than two orders of magnitude and at $P \approx 6,7\text{ GPa}$ reaches saturation. At depressurization, hysteresis is also observed.

In the saturation region, the carrier concentration $\rho \approx 7.5 \cdot 10^{20}\text{ cm}^{-3}$, which is characteristic of metals. The values of Hall coefficient before and after pressure application do not coincide, which supports the conclusion that in $p\text{-CdSb} + 3\% \text{ MnSb}$ irreversible semiconductor-to-metal phase transition occurred. At depressurization, hysteresis is observed.

Fig. 4b shows barometric dependencies of concentration $p(P)$ and mobility $\mu(P)$ at room temperatures. It is seen from Fig. 5 that at atmospheric pressure $p \approx 3.7 \cdot 10^{18}\text{ cm}^{-3}$ and up to pressures $P \approx 1.4\text{ GPa}$ is nearly constant. Then with pressure increasing, p also increases and at $P = 7\text{ GPa}$ reaches saturation. In the saturation region $p = 7.5 \cdot 10^{20}\text{ cm}^{-3}$, which once again supports the conclusion about phase transition being semiconductor-metal.

The mobility value μ that at atmospheric pressure is equal to $17.3\text{ cm}^2/\text{V}\cdot\text{s}$ decreases with pressure increasing and in the minimum at $P = 4.2\text{ GPa}$ equals $1\text{ cm}^2/\text{V}\cdot\text{s}$, i.e. becomes lower by 17-fold. Then mobility increases again and at $P \geq 7\text{ GPa}$ becomes greater by 2 orders of magnitude and reaches saturation.

By using experimental values of the origin P_b and the end of the phase transition P_e , at pressure elevation and depressurization P'_b, P'_e according to the ideas given in [18-23] and the procedure proposed in [20] some characteristic points and phase transformation parameters at high pressure have been calculated.

Table 1 – Parameters characterizing phase transition at high pressures in $p\text{-CdSb} + \text{MnSb}$ (3 % Mn)

P_b , GPa	P_e , GPa	P_o , GPa	P_{om} , GPa	$P_{h.f.}$, GPa	$P_{b'}$, GPa	$P_{e'}$, GPa	$P_{o'}$, GPa	P_{om} , GPa	$P_{h.f.}$, GPa	$P_{h.t}$, GPa
2.9	7.2	1.9	5.0	4.3	0.9	0.1	3.6	0.5	0.8	4.5

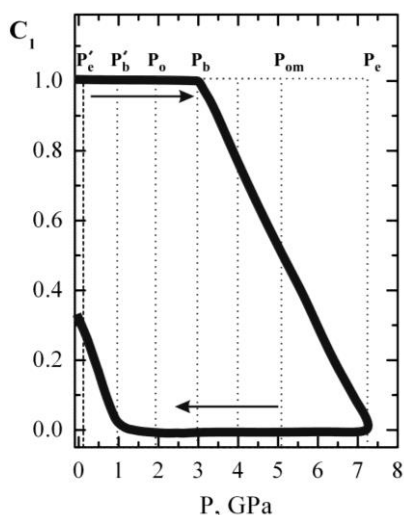


Fig. 5 – Volume fraction of the initial phase C_1 as a function of pressure at compression and decompression for p -CdSb + MnSb (3 % Mn)

From the model heterophase structure – effective medium [19], we have calculated dynamics of changes in the volume fraction of the initial phase C_1 versus pressure. At $P_H - C_1 = 1$ and $C_2 = 0$ and at $P_K - C_1 = 0$ and $C_2 = 1$. Here C_1 and C_2 are relative volumes of

phases $C_1 = V_1/(V_1 + V_2)$, $C_2 = V_2/(V_1 + V_2)$, $C_1 + C_2 = 1$, where V_1 is the initial phase volume, V_2 is the volume of the produced phase. Depicted in Fig. 5 is the dependence of the volume fraction of the initial phase $C_1(P)$ on the pressure at its elevation and depressurization for the sample p -CdSb + 3 % MnSb. It should be noted that the ratio of C_1 before the cycle of pressure application and after is in qualitative agreement with the ratio of Raman spectra intensities (Fig. 3). After pressure application, both the values of C_1 and spectrum intensity decrease.

4. CONCLUSION

Measurements of structural features, Raman spectra, Hall's coefficient and specific resistance at pressure elevation and depressurization at room temperatures in p -CdSb + 3 % MnSb composite have revealed an irreversible structural phase transition. Barometric dependencies of mobility and carrier concentration have been calculated. From the model heterophase structure- effective medium, characteristic points and parameters of phase transition, and also the volume of the initial phase C_1 as a function of pressure have been computed.

The reported study was funded in part by RFBR according to the research project No 13-02-01105-a.

REFERENCES

- V.A. Ivanov, T.G. Aminov, V.M. Novotortsev, V.T. Kalinnikov, *Russ. Chem. Bull.* **53**, 2357 (2004).
- A.V. Kochura B. Aronzon, K.G. Lisunov, A.V. Lashkul, A. Sidorenko, R. De Renzi, S.F. Marenkin, M. Alam, A.P. Kuzmenko, E. Lahderanta, *J. Appl. Phys.* **113**, 083905 (2013).
- S.F. Marenkin, V.M. Trukhan, I.V. Fedorchenko, T.V. Shoulkavaya, *Russ. J. Inorg. Chem.* **59**, 355 (2014).
- A.V. Kochura, S.F. Marenkin, A.D. Izotov, P.N. Vasil'ev, P.V. Abakumov, A.P. Kuzmenko, *Inorg. Mater.* **51**, 754 (2015).
- A.Yu. Mollaev, *Fizika i Tehnika Visokikh Davlenii* **14**, 34 (2004).
- A.Yu. Mollaev, L.A. Saipulaeva, R.K. Arslanov, A.N. Babushkin, *Inorg. Mater.* **50**, 861 (2014).
- A.Yu. Mollaev, R.K. Arslanov, R.G. Dzhamedov, S.F. Marenkin, S.A. Varnavskii, *Inorg. Mater.* **41**, 217 (2005).
- A.Yu. Mollaev, R.K. Arslanov, R.G. Dzhamedov, S.F. Marenkin, S.A. Varnavskii, *Fizika i Tehnika Visokikh Davlenii* **14**, 132 (2004).
- L.G. Khvostantsev, L.P. Vereshagin, A.P. Novikov, *High Temp. High Pressure* **9**, 637 (1977).
- A.Yu. Mollaev, L.A. Saipulaeva, R.K. Arslanov, S.F. Marenkin, *Inorg. Mater.* **37**, 327 (2001).
- G.J. Piermarini, S. Block, J.D. Barnett, *J. Appl. Phys.* **44**, 5377 (1973).
- V.M. Novotortsev, A.V. Kochura, S.F. Marenkin, I.V. Fedorchenko, S.V. Drogunov, A. Lashkul, E. Lahderanta, *Russ. J. Inorg. Chem.* **56**, 1951 (2011).
- W.J. Takei, D.E. Cox, G. Shirane, *Phys. Rev.* **129**, 2008 (1963).
- I. Teramoto, A.M.J.G. Van Run, *J. Phys. Chem. Solids* **29**, 347 (1968).
- D. Houde, J. Lefavre, S. Jandl, E. Arushanov, *Sol. St. Comm.* **41**, 325 (1982).
- D.M. Triches, S.M. Souza, J.C. de Lima, T.A. Grandi, C.E.M. Campos, A. Polian, J.P. Ltie, F. Baudelet, J.C. Chervin, *J. Appl. Phys.* **106**, 013509 (2009).
- D.V. Smirnov, D.V. Mashovets, S. Pasquier, J. Leotin, P. Puech, G. Landa, Yu.V. Roznovan, *Semicond. Sci. Technol.* **9**, 333 (1994).
- A.L. Roitburd, *Phys.-Usp.* **17**, 326 (1974).
- A.L. Roitburd, *Phys. Solid State* **25**, 33 (1983).
- A.Yu. Mollaev, R.K. Arslanov, R.I. Akhmedov, L.A. Saipulaeva, *Fizika i Tehnika Visokikh Davlenii* **4**, 66 (1994).
- A.L. Roitburd, *Phys. Solid State* **26**, 2025 (1984).
- V.N. Kozlov, G.R. Umarov, A.A. Firsov, *Fizika i Tehnika Visokikh Davlenii* **23**, 9 (1986).
- M.I. Daunov, A.B. Magomedov, A.Yu. Mollaev, S.M. Salikhov, L.A. Saipulaeva, *Sverkhverdye Materialy* **3**, 3 (1992).